Dynamics of Downwelling in an Eddy-Resolving Convective Basin

MICHAEL A. SPALL

Woods Hole Oceanographic Institution, Woods Hole, Massachusetts

(Manuscript received 11 March 2010, in final form 14 May 2010)

ABSTRACT

The mean downwelling in an eddy-resolving model of a convective basin is concentrated near the boundary where eddies are shed from the cyclonic boundary current into the interior. It is suggested that the buoyancy-forced downwelling in the Labrador Sea and the Lofoten Basin is similarly concentrated in analogous eddy formation regions along their eastern boundaries. Use of a transformed Eulerian mean depiction of the density transport reveals the central role eddy fluxes play in maintaining the adiabatic nature of the flow in a nonperiodic region where heat is lost from the boundary current. The vorticity balance in the downwelling region is primarily between stretching of planetary vorticity and eddy flux divergence of relative vorticity, although a narrow viscous boundary layer is ultimately important in closing the regional vorticity budget. This overall balance is similar in some ways to the diffusive–viscous balance represented in previous boundary layer theories, and suggests that the downwelling in convective basins may be properly represented in low-resolution climate models if eddy flux parameterizations are adiabatic, identify localized regions of eddy formations, and allow density to be transported far from the region of eddy formations.

1. Introduction

Buoyancy-forced downwelling of waters is a fundamental component of the oceanic three-dimensional circulation. This downwelling is part of the meridional overturning circulation, which plays an important role in the global climate system. It has recently become apparent that the sinking of dense waters at high latitudes that results from buoyancy loss to the atmosphere takes place near lateral boundaries, often far from the regions in the ocean interior where deep convection takes place (Marotzke and Scott 1999; Spall 2003; Pedlosky 2003; Cessi and Wolfe 2009). For stratified flows adjacent to a vertical wall, our current theoretical understanding is that downwelling is concentrated in a viscous–diffusive boundary layer whose width scales as $\sigma^{1/2}L_d$, where σ is a horizontal Prandtl number and L_d is the internal deformation radius (Barcilon and Pedlosky 1967, hereafter BP67; Spall 2003; Pedlosky 2003). The width of this theoretical boundary layer is controlled by coupled balances in the density and vorticity equations. Horizontal diffusion of density is balanced by vertical advection of the mean stratification. This vertical advection gives rise to the stretching of planetary vorticity in the vorticity equation, which is balanced by horizontal diffusion of relative vorticity into the boundary. This interplay gives rise to the dependence on the horizontal Prandtl number.

The recent idealized wind- and buoyancy-forced modeling study by Cessi and Wolfe (2009) found that downwelling in the stratified part of the water column near the eastern boundary was also important for maintenance of the subtropical thermocline. Although their focus was on the dynamics of the narrow sublayer inside the deformation-scale eastern boundary current, they also demonstrated that resolved, not parameterized, eddy fluxes played a central role in both the momentum and density equation balances, and were essential to satisfy the eastern boundary condition.

Repeat hydrographic sections across the Labrador Sea, combined with absolute velocity measurements, indicate that the maximum downwelling transport in the area north of the AR7W section (approximately 57°N) is 10^6 m^3 s^{-1} at 800-m depth, and that downwelling extends as deep as 1500 m (Pickart and Spall 2007). It was also found that the downwelling of waters convectively modified in the interior of the Labrador Sea occurs somewhere near the boundary within the stratified part of the water column, in general agreement with the theory of BP67.

Corresponding author address: Michael Spall, WHOI, MS 21, 360 Woods Hole Rd., Woods Hole, MA 02543.
E-mail: mspall@whoi.edu

DOI: 10.1175/2010JPO4465.1

While the boundary layer theory for downwelling in stratified flows by BP67, and its applications in Spall (2003) and Pedlosky (2003), depends on the diapycnal mixing of density due to horizontal diffusion, diapycnal mixing in the ocean is generally weak. The aim of the present study is to explore downwelling in a convective basin with very small explicit diffusion of density, with particular interest in the aspects of this process that would need to be properly parameterized in low-resolution climate models in order to accurately represent this component of the downwelling limb of the thermohaline circulation.

2. An eddy-resolving ocean model with downwelling

The numerical model used in this study is the Massachusetts Institute of Technology (MIT) general circulation model (Marshall et al. 1997), which solves the hydrostatic, primitive equations on a staggered C-grid with level vertical coordinates. The model domain consists of an elongated basin subject to cooling at the surface, which is connected to a smaller rectangular region through a strait (Fig. 1). The domain has topography along the perimeter that slopes exponentially from the surface down to the bottom depth of 3000 m with a horizontal e-folding scale that varies from 40 km over most of the basin to 10 km along the eastern boundary between $y = 400$ km and $y = 700$ km. The Coriolis parameter varies linearly with y as $f = f_0 + \beta y$, where $f_0 = 1 \times 10^{-4}$ s^{-1}, $\beta = 2 \times 10^{-11}$ m^{-1} s^{-1}, and y is the distance from the model southern boundary. The meridional gradient in planetary vorticity is included here, although the material results are not sensitive to it. The eastern boundary is distinct in these calculations because of the local topography, not because of β. The model is forced by applying 50 W m^{-2} uniform cooling at the surface over the northern basin and by restoring toward a temperature profile with uniform vertical stratification of $N^2 = (g/\rho_0)\partial\rho/\partial z = 10^{-6}$ s^{-2} in the southern rectangular region. This gives a first baroclinic deformation radius, based on the full ocean depth, of $L_d = NH/f_0 = 30$ km.

The vertical grid spacing is 100 m over the full depth of 3000 m (30 levels). The model has variable horizontal grid spacing, as indicated in Fig. 1. The grid spacing in the region along the eastern boundary is 1 km. The model was first spun up for a period of 20 years with a slightly lower resolution grid (the region of 1-km grid spacing was 2 km). The temperature, velocity, and sea surface height fields at the end of this calculation were then interpolated onto the finer grid to initialize the final 200-day calculation used in the analysis below.

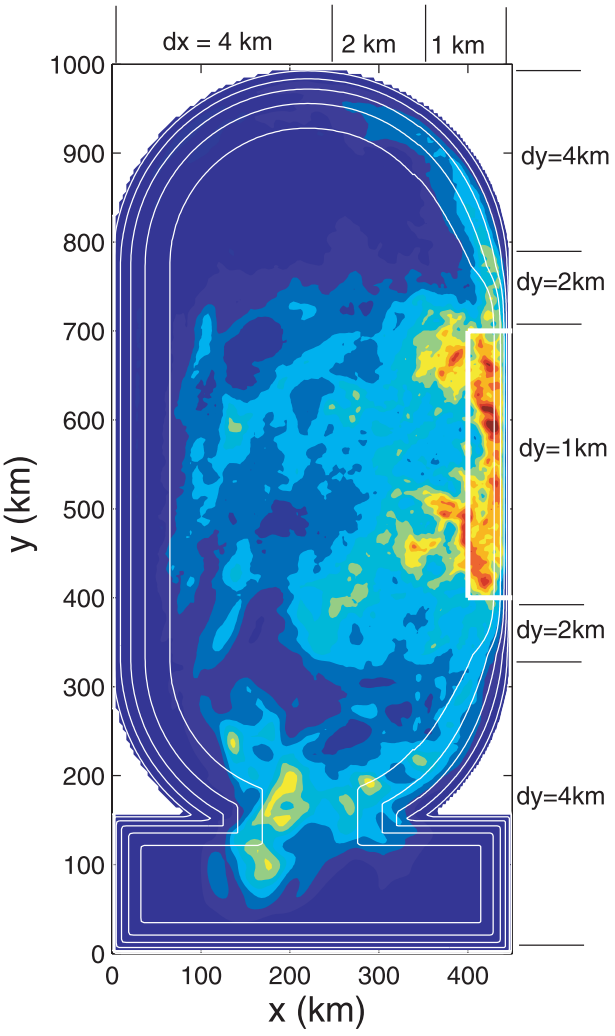

FIG. 1. Eddy kinetic energy (maximum ≈500 cm^2 s^{-2}, contour interval is 50 cm^2 s^{-2}) over the model domain from the high-resolution calculation. Topography is indicated by the thin white contours (contour interval is 500 m). The analysis region is marked by the bold white box along the eastern boundary. (top) Zonal and (right) meridional grid spacings.

The model incorporates second-order vertical viscosity and diffusivity with coefficients 10^{-5} m^2 s^{-1}. The vertical diffusion is increased to 1000 m^2 s^{-1} for statically unstable conditions in order to represent vertical convection. Horizontal viscosity is parameterized as a second-order operator with the coefficient A_h determined by a Smagorinsky (1963) closure as $A_h = (\nu_s/\pi)^2 L^2[(u_x - v_y)^2 + (u_y + v_x)^2]^{1/2}$, where $\nu_s = 2.5$ is a nondimensional coefficient, L is the grid spacing, and u and v are the horizontal velocities (subscripts indicate partial differentiation). Temperature is advected with a third-order direct space–time flux-limiting scheme. There is no explicit horizontal diffusion of temperature.

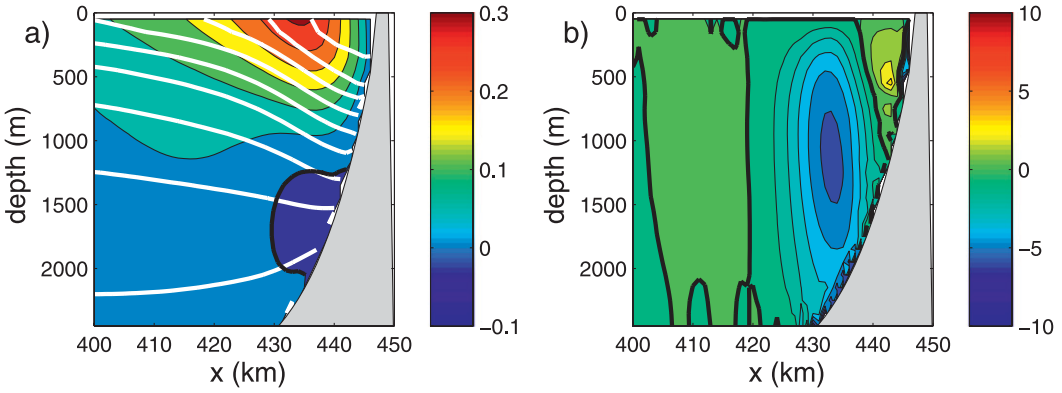

FIG. 2. Mean x-depth sections averaged over 200 days and between $y = 400$ km and $y = 700$ km. (a) Meridional velocity (colors, m s^{-1}) and temperature (white contours, contour interval 0.1°C) and (b) vertical velocity (10^{-4} m s^{-1}). The bold black line marks the zero contour in (a) and (b).

Density is linearly related to temperature with a thermal expansion coefficient of -0.2 kg m^{-3} °C^{-1}.

The basin-scale circulation consists of a warm, cyclonic boundary current that enters the cooling basin along the eastern side of the strait and exits the basin along the western side of the strait. The boundary current accelerates over the region of steep topography, which results in enhanced instability and eddy formation compared to the rest of the domain where the topographic slope is weaker (Katsman et al. 2004; Wolfe and Cenedese 2006; Bracco et al. 2008; Spall 2010). This is reflected in the eddy kinetic energy (Fig. 1), which takes on a maximum value in the region of steep topography and has high values extending into the basin interior as a result of eddy shedding from the boundary current. Similar regions of enhanced eddy kinetic energy adjacent to steep topography are found along the eastern boundaries of the Labrador Sea (Prater 2002) and Lofoten Basin in the Nordic Seas (Poulain et al. 1996).

Vertical sections of the meridional average of the 200-day time-mean meridional velocity and temperature within the white box in Fig. 1 are shown in Fig. 2a. The mean boundary current is approximately 30 km wide with a maximum velocity just over 30 cm s^{-1}. The mean horizontal velocity is essentially parallel to the boundary; there is very little mean flow between the boundary region and the interior.

The time-mean Eulerian vertical velocity is small everywhere in the cooling basin except along the region of steep topography and eddy activity. A meridional average of the vertical velocity in the analysis box is shown in Fig. 2b. Over 95% of the total downwelling in the basin is concentrated in this relatively narrow band of O(20 km) width along the eastern boundary, where the eddies are formed. The maximum downwelling transport of 1.8×10^6 m^3 s^{-1} is located at 1100-m depth.

The importance of eddy fluxes in the region of downwelling is indicated by the flux divergence of the advective terms in the temperature tendency equation shown in Fig. 3. The advective terms essentially balance at all depths, indicating that local surface cooling does not penetrate below 100 m in the boundary current and that diffusive effects are small. The mean advection is acting to warm the region throughout the water column. This represents the inflow of warm water in the cyclonic boundary current. Anticyclonic eddies transport warm water from the boundary current into the interior and act to cool the region at all depths (as shown in Fig. 6). Similar warm anticyclones are observed to be formed along the eastern boundaries of the Labrador Sea and the Lofoten Basin (Lilly and Rhines 2002; Poulain et al.

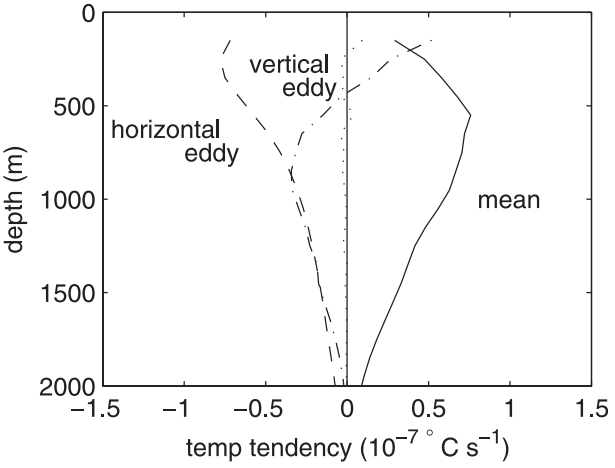

FIG. 3. Advective influences on the temperature tendency as a function of depth averaged over the white box in Fig. 1. (solid line) Mean flux divergence; (dashed line) horizontal eddy flux divergence; (dotted–dashed line) vertical eddy flux divergence; and (dotted line) sum of advective flux divergences.

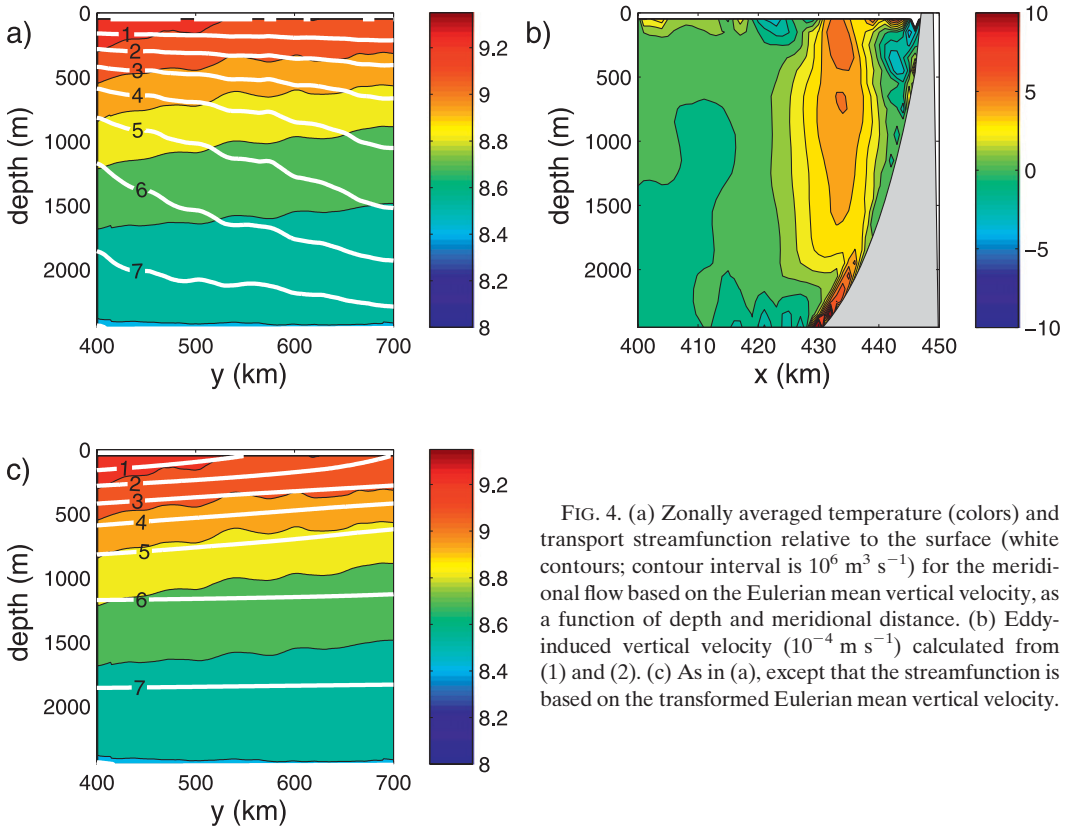

FIG. 4. (a) Zonally averaged temperature (colors) and transport streamfunction relative to the surface (white contours; contour interval is 10^6 m^3 s^{-1}) for the meridional flow based on the Eulerian mean vertical velocity, as a function of depth and meridional distance. (b) Eddy-induced vertical velocity (10^{-4} m s^{-1}) calculated from (1) and (2). (c) As in (a), except that the streamfunction is based on the transformed Eulerian mean vertical velocity.

1996). The vertical eddy fluxes cool the deep ocean and warm the upper ocean. This is consistent with baroclinic instability, which releases potential energy by upwelling warm water and downwelling cool water (analysis of the energy conversion terms confirms baroclinic instability is active).

3. Dynamics of downwelling

The mean temperature and northward transport between 400 km and the boundary is shown in Fig. 4a. The temperature in the boundary current decreases at all depths as one moves northward, as expected since the boundary current loses heat as a result of eddy exchange with the interior. The mean along-boundary transport deepens, but does not decrease, as the boundary current flows northward as a result of the downward mean vertical velocity. If eddies were not important for the heat budget, this would require an unrealistically large diapycnal mixing coefficient of $\mathcal{O}(10^{-2}$ m^2 s$^{-1})$ to balance this cross-isotherm mean advection.

The influence of eddies on density advection can be represented in compact form by considering the transformed Eulerian mean formulation (e.g., Andrews and McIntyre 1978). This representation includes the effects of eddy fluxes, but written in such a way that they appear as an advection acting on the mean density field. If it is assumed that the eddy advection of density is adiabatic, then these eddy-induced cross-front and vertical velocities may be written in the form of a streamfunction (where subscripts indicate partial differentiation) as

$$\tilde{u} = -\Psi_z, \quad \tilde{w} = \Psi_x. \tag{1}$$

There are numerous choices for the streamfunction Ψ as reviewed, for example, by Vallis (2006, 304–314). For the primitive equations, a convenient choice is

$$\Psi = -\frac{\overline{u'\rho'}\overline{\rho}_z - \overline{w'\rho'}\overline{\rho}_x}{\overline{\rho}_x^2 + \overline{\rho}_z^2}, \tag{2}$$

where the overbar indicates a time average and the primed variables are deviations from the mean. The eddy flux is dominated by the zonal component, $(\overline{v'\rho'})_y \ll (\overline{u'\rho'})_x$ and $\overline{\rho}_{zy} \ll \overline{\rho}_{zx}$, so the meridional eddy flux term is neglected.

The streamfunction in (2) was calculated at each grid point in the analysis box and then averaged in the meridional direction to yield a two-dimensional depiction of the eddy-induced velocity. The time-averaged terms are only weakly dependent on latitude, so this averaging is used to reduce the influence of synoptic variability in

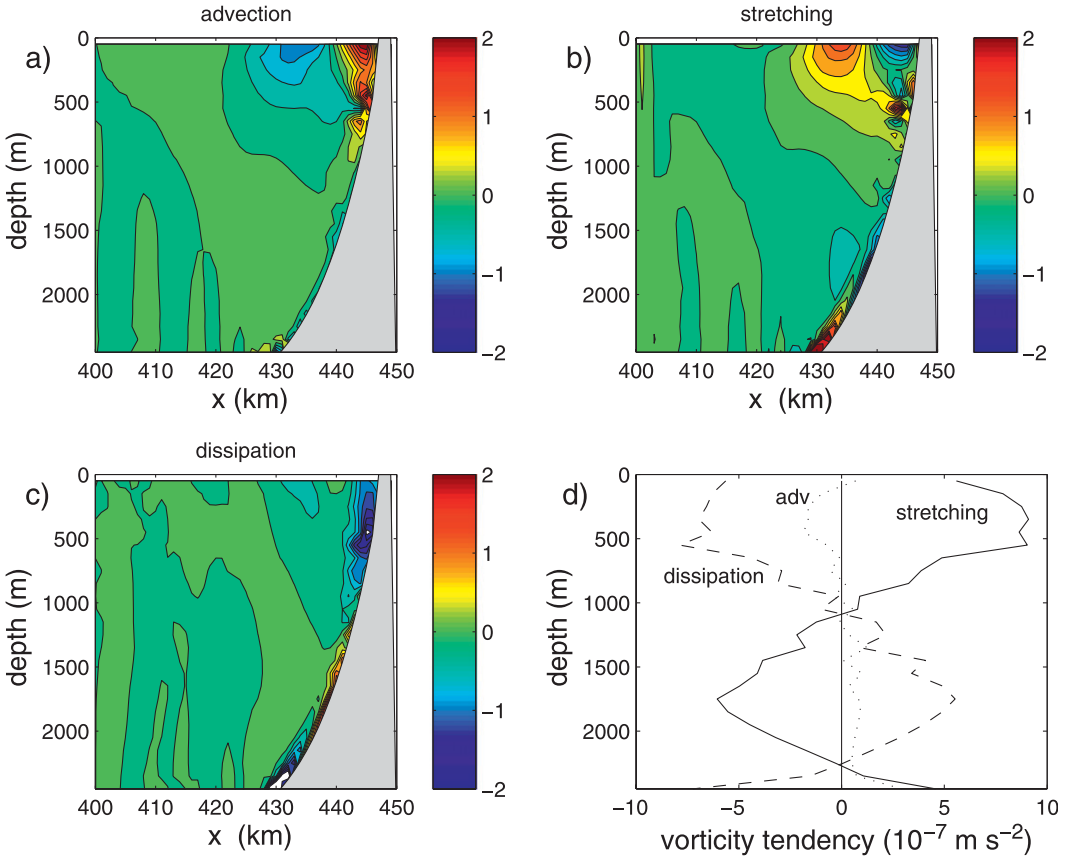

FIG. 5. Meridionally and temporally averaged terms in the relative vorticity Eq. (3), units 10^{-10} s^{-2}. (a) Advection; (b) stretching of planetary vorticity; (c) dissipation; and (d) zonal integral of the terms in (a),(b), and (c) (10^{-7} m s^{-2}).

Ψ. The effective eddy-induced vertical velocity $\tilde{w}$ calculated from this averaged streamfunction via (1) is shown in Fig. 4b. It is nearly equal in magnitude and opposite in sign to the Eulerian mean vertical velocity in Fig. 2b. Such an upward eddy heat flux is consistent with Fig. 3 and baroclinic instability. An along-boundary transport streamfunction was calculated using the zonally averaged residual vertical velocity (the sum of sections in Figs. 2b and 4b). This results in upwelling that is in general agreement with the rise of the mean isopycnals (Fig. 4c), indicating that the flow is nearly adiabatic.

The question remains as to what balances the mean Eulerian vertical velocity in the vertical component of the relative vorticity equation, written below as the sum of three groups of terms:

$$\zeta_t = \underbrace{\frac{-\boldsymbol{v}\cdot\nabla\zeta - w\zeta_z - \nabla w\cdot\boldsymbol{v}_z + \zeta w_z - \beta v}{\text{advection}}}_{\text{advection}} + \underbrace{\frac{fw_z}{\text{stretching}}}_{\text{stretching}} + \underbrace{\frac{A\nabla^2\zeta + K\zeta_{zz}}{\text{dissipation}}}_{\text{dissipation}} \approx 0. \qquad (3)$$

The balance in the boundary layer theory of BP67 is between the last two terms: stretching and dissipation. All three groups of terms have been calculated from the model output and averaged in the meridional direction to produce zonal sections (Fig. 5). The advection term includes all advective effects, including horizontal advection of relative vorticity, vertical advection of relative vorticity, tilting of horizontal vorticity, vertical stretching of relative vorticity, and advection of planetary vorticity.

The strong mean Eulerian downwelling results in stretching of planetary vorticity, fw_z, that tends to increase the upper-ocean relative vorticity in the region of maximum downwelling. This is balanced to a large degree by the advective export of positive vorticity (primarily the horizontal eddy flux divergence of relative vorticity). The majority of the relative vorticity flux is toward the boundary, but there is also an export of positive relative vorticity into the interior (not shown). The flux toward the boundary goes to zero at the boundary because of the no-normal flow boundary condition, giving

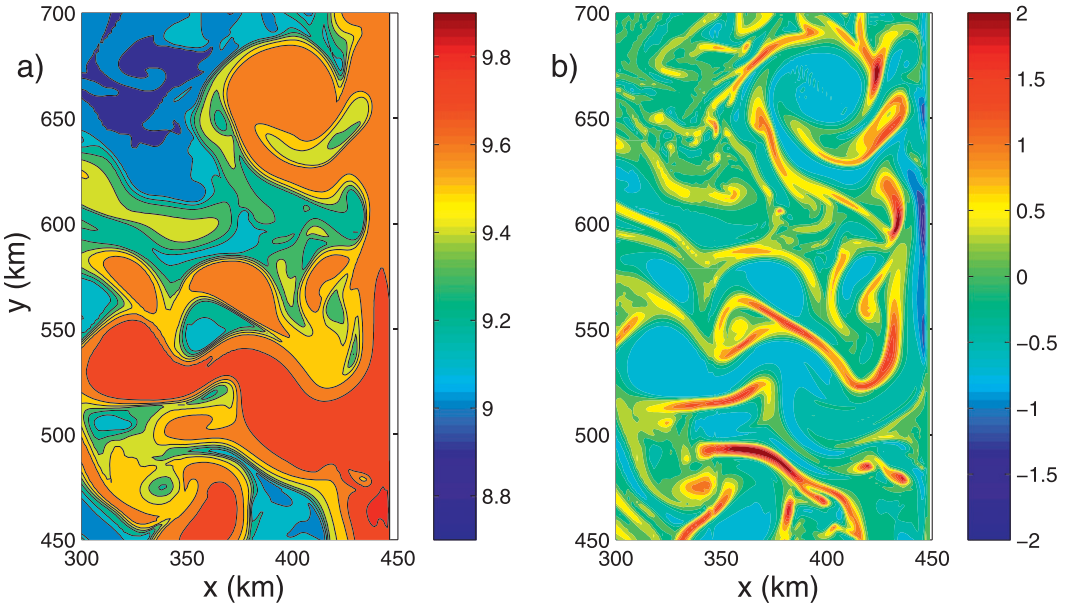

FIG. 6. Snapshot at 50-m depth near the eastern boundary of (a) temperature (contour interval is 0.1°C) and (b) relative vorticity divided by the Coriolis parameter (contour interval is 0.25). The vorticity field is characterized by large, warm, anticyclonic eddies surrounded by narrow filaments of very strong cyclonic vorticity.

rise to a flux convergence (the positive region near the boundary in the upper 700 m) that is primarily balanced by dissipation. Thus, unlike the theory of BP67, the region of dissipation is offset from the region of downwelling, but they are connected through the lateral eddy flux term. The positive relative vorticity flux into the basin interior is somewhat surprising since the dominant form of eddies exported from the boundary current are anticyclonic, and it points to the importance of submesoscale filaments of positive relative vorticity in the eddy field (Fig. 6). The primary balance, when integrated over the whole downwelling region, is between stretching and dissipation, similar to the BP67 balance. However, the positive relative vorticity flux into the interior balances up to 20% of the stretching (Fig. 5d).

4. Discussion

The Eulerian mean vertical velocity is small everywhere in the basin except in the region where eddies are formed from the cyclonic boundary current. This is analogous to the regions of steep topography and eddy shedding found along the eastern boundaries of the Labrador Sea and Lofoten Basin, and so it is expected that the downwelling experienced in these basins is localized to these relatively small segments of the boundary current even though heat loss and convection are spread throughout these basins.

The balance in the downwelling region in the present model with well-resolved mesoscale eddies is different in detail, but similar in character, compared to that represented by the diffusive boundary layer theory of BP67. The primary difference is that the resolved eddy fluxes of density extract heat adiabatically from the boundary current and deposit it far from the boundary in the basin interior, whereas the parameterized boundary layer theory relies on a local parameterization for the eddy flux (and thus its divergence). To be accurately parameterized, the eddy density flux should be adiabatic, reflect the dependence of eddy generation on the local mean velocity field, and nonlocal (meaning that the heat transported by the eddies is lost far from the region of formation). The present vorticity budget indicates that most of the stretching induced by downwelling is ultimately balanced in a narrow viscous boundary layer (similar to the vorticity balance in BP67), although eddy fluxes are required to connect the stretching region to the dissipation region. Nonetheless, the results suggest that the overall vorticity budget may be adequately represented by standard lateral viscosity with a no-slip boundary condition. The flux of relative vorticity into the basin interior, and the important role played by submesoscale filaments of high relative vorticity, will be more difficult to parameterize. These features are only a few kilometers wide and only marginally resolved in the present calculations. It is still an open question as to whether or not these filaments play a more important role in the basin-scale vorticity budget at higher resolution.

Acknowledgments. This study was supported by the National Science Foundation under Grants OCE-0726339 and OCE-0850416. Comments and suggestions from two anonymous reviewers helped to improve the presentation.

REFERENCES

Andrews, D. G., and M. E. McIntyre, 1978: Generalized Eliassen–Palm and Charney–Drazin theorems for waves on axisymmetric mean flows in compressible atmospheres. *J. Atmos. Sci.,* **35,** 175–185.

Barcilon, V., and J. Pedlosky, 1967: A unified theory of homogeneous and stratified rotating fluids. *J. Fluid Mech.,* **29,** 609–621.

Bracco, A., J. Pedlosky, and R. S. Pickart, 2008: Eddy formation near the west coast of Greenland. *J. Phys. Oceanogr.,* **38,** 1992–2002.

Cessi, P., and C. L. Wolfe, 2009: Eddy-driven buoyancy gradients on eastern boundaries and their role in the thermocline. *J. Phys. Oceanogr.,* **39,** 1595–1614.

Katsman, C. A., M. A. Spall, and R. S. Pickart, 2004: Boundary current eddies and their role in the restratification of the Labrador Sea. *J. Phys. Oceanogr.,* **34,** 1967–1983.

Lilly, J. M., and P. B. Rhines, 2002: Coherent eddies in the Labrador Sea observed from a mooring. *J. Phys. Oceanogr.,* **32,** 585–598.

Marotzke, J., and J. R. Scott, 1999: Convective mixing and the thermohaline circulation. *J. Phys. Oceanogr.,* **29,** 2962–2970.

Marshall, J., C. Hill, L. Perelman, and A. Adcroft, 1997: Hydrostatic, quasi-hydrostatic, and non-hydrostatic ocean modeling. *J. Geophys. Res.,* **102,** 5733–5752.

Pedlosky, J., 2003: Thermally driven circulations in small ocean basins. *J. Phys. Oceanogr.,* **33,** 2333–2340.

Pickart, R. S., and M. A. Spall, 2007: Impact of Labrador Sea convection on the North Atlantic meridional overturning circulation. *J. Phys. Oceanogr.,* **37,** 2207–2227.

Poulain, P.-M., A. Warn-Varas, and P. P. Niiler, 1996: Near surface circulation of the Nordic Seas as measured by Lagrangian drifters. *J. Geophys. Res.,* **101,** 18 237–18 258.

Prater, M., 2002: Eddies in the Labrador Sea as observed by profiling RAFOS floats and remote sensing. *J. Phys. Oceanogr.,* **32,** 411–427.

Smagorinsky, J., 1963: General circulation experiments with the primitive equations: I. The basic experiment. *Mon. Wea. Rev.,* **91,** 99–164.

Spall, M. A., 2003: On the thermohaline circulation in flat bottom marginal seas. *J. Mar. Res.,* **61,** 1–25.

——, 2010: Non-local topographic influences on deep convection: An idealized model for the Nordic Seas. *Ocean Modell.,* **32,** 72–85.

Vallis, G. K., 2006: *Atmospheric and Oceanic Fluid Dynamics*. Cambridge University Press, 745 pp.

Wolfe, C. L., and C. Cenedese, 2006: Laboratory experiments on eddy generation by a buoyancy coastal current flowing over variable bathymetry. *J. Phys. Oceanogr.,* **36,** 395–411.